The contributions of individual countries and regions to the global radiative forcing

Bo Fu[a,1], Bengang Li[a,1,2], Thomas Gasser[b], Shu Tao[a], Philippe Ciais[c], Shilong Piao[a,d], Yves Balkanski[c], Wei Li[a], Tianya Yin[a], Luchao Han[a], Yunman Han[a], Siyuan Peng[a], and Jing Xu[a]

[a]Sino-French Institute for Earth System Science, Ministry of Education Key Laboratory for Earth Surface Processes, College of Urban and Environmental Sciences, Peking University, Beijing 100871, China; [b]International Institute for Applied Systems Analysis, 2361 Laxenburg, Austria; [c]Laboratoire des Sciences du Climat et de l'Environnement, Comissariat à l'Energie Atomique et aux Energies Alternatives, Centre National de la Recherche Scientifique, Université de Versailles St Quentin en Yvelines, 91191 Gif-sur-Yvette, France; and [d]Key Laboratory of Alpine Ecology, Center for Excellence in Tibetan Earth Science, Institute of Tibetan Plateau Research, Chinese Academy of Sciences, Beijing 100864, China

Edited by Christopher B. Field, Stanford University, Stanford, CA, and approved February 8, 2021 (received for review August 30, 2020)

Knowing the historical relative contribution of greenhouse gases (GHGs) and short-lived climate forcers (SLCFs) to global radiative forcing (RF) at the regional level can help understand how future GHGs emission reductions and associated or independent reductions in SLCFs will affect the ultimate purpose of the Paris Agreement. In this study, we use a compact Earth system model to quantify the global RF and attribute global RF to individual countries and regions. As our evaluation, the United States, the first 15 European Union members, and China are the top three contributors, accounting for 21.9 ± 3.1%, 13.7 ± 1.6%, and 8.6 ± 7.0% of global RF in 2014, respectively. We also find a contrast between developed countries where GHGs dominate the RF and developing countries where SLCFs including aerosols and ozone are more dominant. In developing countries, negative RF caused by aerosols largely masks the positive RF from GHGs. As developing countries take measures to improve the air quality, their negative contributions from aerosols will likely be reduced in the future, which will in turn enhance global warming. This underlines the importance of reducing GHG emissions in parallel to avoid any detrimental consequences from air quality policies.

radiative forcing | climate change | attribution | regional contributions

Anthropogenic activities have been the main drivers of climate change since industrialization, and recent climate change has had substantial impact on both humans and natural systems (1). Increase in anthropogenic greenhouse gas (GHG) emissions is the dominant cause of observed climate warming, and those emissions are driven by the energy demand from economic and population growth since the preindustrial era. In addition to GHGs, anthropogenic activities also change the climate through aerosol emissions, such as black carbon (BC) and organic aerosols (both primary and secondary), as well as aerosol and ozone precursor emissions such as SO_2, NH_3, NO_X, VOC, and CO, all of which are termed short-lived climate forcers (SLCFs). Albedo changes are another climate forcer, mainly induced by land-cover change (LCC). Radiative forcing (RF), a natural or anthropogenic perturbation to the earth's energy budget, is used to quantify the magnitude by which forcers like GHGs and SLCFs change the climate (2).

The Paris Agreement, for the first time, brings all nations into a common cause to undertake ambitious efforts to combat climate change and adapt to its effects. Its goal is to limit global warming to well below 2 °C, preferably to 1.5 °C, compared to preindustrial levels. To achieve this goal, individual signatory countries are requested to submit nationally determined contributions (NDCs) every 5 y. Knowing the historical relative contribution of GHGs and SLCFs to global RF at the regional level can help understand how future GHGs emission reductions and associated or independent reductions in SLCFs will affect the ultimate purpose of the Paris Agreement. Since NDCs are submitted without negotiations and given that stock takes of global emissions and commitments are planned in 2023 and 2028 to assess progress toward the Paris Agreement climate goals, it is even more essential to monitor the contributions of individual countries to climate change.

Quantifying the individual country and regional historical contributions to global RF was suggested years ago in the Brazilian Proposal (3) to follow the principle of common but differentiated responsibilities and respective capabilities established by the United Nations Framework Convention on Climate Change (UNFCCC). The Copenhagen Conference of Parties in 2009 marked a shift away from this top-down approach, which meant to attribute mitigation responsibilities relatively to each country's historical contribution to global climate change, and instead all parties involved in the Paris Agreement in 2016 agreed to take a bottom-up approach yet with a global stock take and a process to improve bottom-up intentions of mitigation.

In this study, we quantify individual countries' and regional contributions to the global RF, following a method close to the one established in our previous estimation for China (3). Compared to this previous work, secondary organic aerosols (SOA), aerosol–cloud interaction, and albedo change induced by BC deposition on snow are included in this study, making it more systematic and comprehensive, albeit at the cost of using a simplified model leading to increased uncertainty. The global RFs are calculated using the reduced-complexity Earth system model OSCAR

Significance

Radiative forcing (RF) is commonly used to describe the change in net radiative flux because of external drivers. Climate change is caused by human activities of all countries, and mitigating climate change requires global joint efforts. It is important to attribute global RF to country scale. At present, developed countries still have greater responsibilities for climate change. Meanwhile, the contribution of developing countries has increased. It is worth noting that the emissions of developing countries include a large amount of negative RF components such as aerosols, masking RF because of greenhouse gases significantly. However, negative RF components in developing countries will be reduced for air quality in the future, which will affect the ultimate purpose of the Paris Agreement.

Author contributions: B.L., T.G., and P.C. designed research; B.F., B.L., and W.L. performed research; B.F., S. Piao, W.L., S. Peng, and J.X. analyzed data; and B.F., B.L., T.G., S.T., P.C., S. Piao, Y.B., T.Y., L.H., and Y.H. wrote the paper.

The authors declare no competing interest.

This article is a PNAS Direct Submission.

[1]B.F. and B.L. contributed equally to this work.

[2]To whom correspondence may be addressed. Email: libengang@pku.edu.cn.

This article contains supporting information online at https://www.pnas.org/lookup/suppl/doi:10.1073/pnas.2018211118/-/DCSupplemental.

Published April 5, 2021.

v3.1, enabled by more complex Earth system models (ESMs) upon which its parameters are calibrated (4–6). The individual countries' or regional contributions are isolated by using factorial simulations in which a small fraction of each country's or region's emissions are removed to quantify their marginal effect on the climate system. This attribution method is used in previous studies (3, 7–9), which is referred to as the "normalized marginal attribution method" (see *Methods* for details).

Results

Global RF Induced by the 15 Regions. We first estimate global anthropogenic RF induced by all components (Table 1) using OSCAR v3.1 and constrained global RF by the estimation in the Intergovernmental Panel on Climate Change Fifth Assessment Report (IPCC AR5) (2). At present day [2014, as in Coupled Model Intercomparison Project Phase 6 (CMIP6) (10)], the total global anthropogenic RF is 2.56 ± 0.58 W/m^2, with carbon dioxide (CO_2) inducing the largest positive contribution, 1.91 ± 0.24 W/m^2 (Fig. 1*A*). CH_4 is the second largest GHG component, with 0.50 ± 0.07 W/m^2 from direct greenhouse effect and 0.07 ± 0.01 W/m^2 from stratospheric water vapor increase. Contributions of tropospheric ozone (O_3t) and BC aerosols are also noticeable, accounting for 0.40 ± 0.05 W/m^2 and 0.62 ± 0.31 W/m^2, respectively. Negative RF are mainly induced by scattering aerosols, aerosol–cloud interactions, and albedo change induced by LCC. Sulfate, primary organic aerosols (POA), and nitrate contribute −0.40 ± 0.24 W/m^2, −0.30 ± 0.20 W/m^2, and −0.11 ± 0.06 W/m^2, respectively. Aerosol–cloud interactions induce −0.46 ± 0.24 W/m^2, which represents almost one-third of the total negative RF. The albedo change induced by LCC induce −0.14 ± 0.07 W/m^2. It should be clarified that RF_{lcc} here refers to only the albedo effect of LCCs (Table 1), and CO_2 emissions from LCCs are accounted for in RF_{CO_2}. At the global scale, the total negative RF (cooling effect, −1.52 ± 0.41 W/m^2) masks 37.3 ± 10.0% of the total positive RF (warming effect, 4.08 ± 0.40 W/m^2).

The global RF are attributed to 15 countries and regions (*SI Appendix*, Table S1). Their relative and absolute contributions to the present-day global RF are shown in Fig. 1*B*, and the uncertainties of RF attributed to the regions can be found in *SI Appendix*, Table S2. The United States contributes 21.9 ± 3.1% (0.56 ± 0.08 W/m^2 out of 2.56 ± 0.58 W/m^2) of the current net global RF from anthropogenic emissions since 1850. The first 15 European Union members (EU15), the Middle East and Africa (MAF), China (CHN), and Russia (RUS) rank second to fifth and contribute 13.7 ± 1.6%, 12.5 ± 6.6%, 8.6 ± 7.0%, and 8.2 ± 2.1% to the current global RF, respectively. Note that MAF is the third largest contributor to global RF. However, this region consists of more than 60 countries, and contributions of individual countries in it are relatively small. Other individual countries with significant contributions are India (IND, 6.2 ± 3.4%), Brazil (BRA, 3.5 ± 2.0%), Japan (JPN, 3.9 ± 0.6%), and Canada (CAN, 1.5 ± 0.5%).

The contribution of each individual country or region is the net of positive and negative RF (Fig. 1*C*). For all countries and regions, CO_2 contributes the most to positive RF, though CH_4 and O_3t are also important positive contributors. Halogenated compounds also noticeably contribute to positive RF in the following developed countries and regions: the United States, EU15, and JPN. Comparatively, BC induces significant positive RF in developing countries such as CHN, IND, and MAF. In terms of negative RF, sulfate aerosols, POA, and related aerosol–cloud interaction contributed the most in CHN, MAF and INDs. The RF_{SO_4},RF_{POA}, and RF_{cloud} are also noticeable in the United States, EU15, BRA, RUS, and Indonesia (IDN). The albedo effect of LCC (RF_{lcc}) in different regions are positive or negative. It is positive in MAF and IND warming the earth, while it is negative in CHN, the United States, BRA, and Australia and New Zealand (ANUZ). According to LCC data from Harmonization of global land use scenarios 2 (LUH2) (11–13) (*SI Appendix*, Fig. S3), negative RF_{lcc} is mainly due to albedo increase caused by deforestation, while LCC from nonforest natural vegetation to cropland leads to a decrease of albedo and positive RF_{lcc}. It is striking to note that developing countries have proportionally greater negative RF than positive RF compared to developed countries. The compensation between positive and negative RF explains their low net RF and small relative contribution to the current global RF. For instance, the United States contributes 17.2 ±1.5% (0.70 ± 0.06 out of 4.08 ± 0.40 W/m^2) of the global positive RF but only 9.2 ± 3.3% (−0.14 ± 0.05 out of −1.52 ± 0.41 W/m^2) of the global negative RF. In contrast, CHN contributes 17.4 ± 2.7% (0.71 ± 0.11 out of 4.08 ± 0.40 W/m^2) of the global positive RF and 32.2 ± 9.2% (−0.49 ± 0.14 out of −1.52 ± 0.41 W/m^2) of the global negative RF. Thus, the relative contribution to the net global RF of the United States is much higher than that of CHN (21.9 ± 3.1% versus 8.6 ± 7.0%), even more than doubled, despite close positive contributions.

Time Series of RF Induced by the Top Three Contributors: The United States, EU15, and CHN. We present historical time series of the absolute and relative contributions to the global RF of these top three regions (Fig. 2) and the other regions (*SI Appendix*, Fig. S1). During the period of 1850 to 2014, their contributions were dominated by RF of CO_2, sulfate aerosols, and aerosol–cloud interaction. In the United States, the absolute contribution of

Table 1. The global anthropogenic RF components in this study

RF induced by all components	Symbol in this study
CO_2	RF_{CO_2}
Methane (CH_4)	RF_{CH_4}
Nitrous oxide (N_2O)	RF_{N_2O}
Halogenated compounds	RF_{Xhalo}
Stratospheric vapor (H_2Os)	RF_{H_2Os}
Sulfate (SO_4)	RF_{SO_4}
Nitrate (NO_3)	RF_{NO_3}
BC	RF_{BC}
POA	RF_{POA}
SOA	RF_{SOA}
O_3t	RF_{O_3t}
Stratospheric ozone (O_3s)	RF_{O_3s}
Albedo change induced by LLC	RF_{lcc}
Albedo change induced by BC deposition on snow	RF_{BCsnow}
Aerosol–cloud interaction	RF_{cloud}

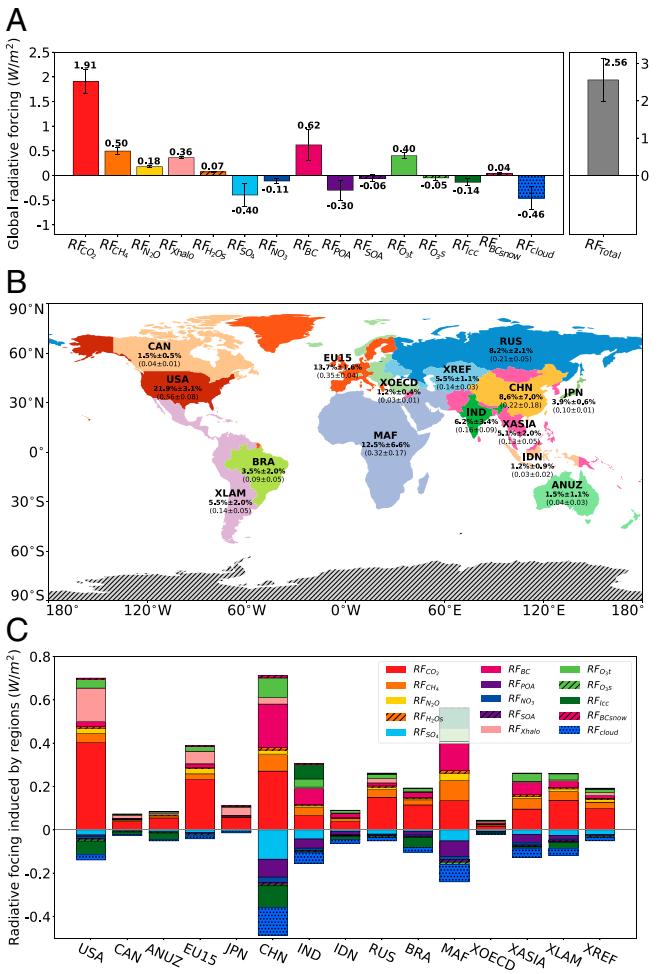

Fig. 1. Present-day (2014) global anthropogenic RF and its attribution to world regions. (*A*) Global RF components and their uncertainties. The total of anthropogenic RF is noted "RF_{Total}" and is shown on the right. (*B*) The 15 countries and regions of the world considered in this study together with their net RF and relative contributions. (*C*) RF composition from these 15 regions. The positive and negative RF are stacked separately. The uncertainties of RF from all regions can be found in *SI Appendix*, Table S2. The values and uncertainties were obtained through Monte Carlo ensembles (n = 3,000). All uncertainties are one SD. The definitions of the RF subscripts in *A* and *C* can be seen in Table 1. The definitions of the regions in *B* and *C* can be seen in *SI Appendix*, Table S1.

CO_2 to global RF has progressively increased since 1850 (up to 0.40 ± 0.06 W/m^2). However, the positive RF induced by halogenated compounds only started increasing sharply after the 1970s (up to 0.15 ± 0.01 W/m^2). In contrast, negative RF induced by aerosols and aerosol–cloud interaction increased between 1850 and 1970 (up to −0.25 ± 0.08 W/m^2). After 1970, the negative RF started being reduced (down to −0.14 ± 0.05 W/m^2) as a result of aerosol controls enacted to improve air quality (14). Overall, the net contribution of the United States to the global RF exhibits an increase from 1850 to present (up to 0.56 ± 0.08 W/m^2), marked by an acceleration after the 1970s. The historical pattern of RF components for EU15 are similar to those for the United States. However, in terms of absolute value, the negative RF increased at a faster rate in EU15, indicating a strengthening cooling effect of aerosols during 1940 to 1970 (from −0.08 ± 0.03 W/m^2 to −0.15 ± 0.06 W/m^2) because of intensive SO_2 emissions in postwar reconstruction, and then reduced more rapidly after the 1970s (from −0.15 ± 0.06 W/m^2 to −0.04 ± 0.01 W/m^2) because of stricter air pollution control (14). Thus, the net contribution of EU15 to the global RF slowly increased before the 1940s (up to 0.12 ± 0.05 W/m^2), remained stable in the 1940 to 1970 period (from 0.12 ± 0.05 W/m^2 to 0.14 ± 0.07 W/m^2), and rapidly increased after the 1970s (up to 0. 39 ± 0.04 W/m^2). The trends of CHN are noticeably different from those of the United States and the EU15. Industrialization in CHN began in the 1900s, and rapid economic growth started in the 1980s as a result of CHN's reforms and open policies (15). Consequently, both positive and negative RF stayed at a very low level until 1900. In 1949, when the People's Republic of China was founded, the positive and negative RF still were as low as +0.09 ± 0.02 W/m^2 and −0.06 ± 0.02 W/m^2, respectively. In the first three decades (1950 to 1980), the increase of the positive and negative RF were +0.17 ± 0.05 W/m^2 and −0.17 ± 0.06 W/m^2 and then rose to +0.44 ± 0.12 W/m^2 and −0.25 ± 0.16 W/m^2 over the following three decades (1980 to 2014). The net contribution of CHN to the global RF stays stable before the 1980s (about 0.03 W/m^2), after which the pace of increase grew rapidly (from 0.03 ± 0.07 W/m^2 to 0.22 ± 0.18 W/m^2). It is important to note that since 1949, the increase in negative RF (from −0.06 ± 0.02 W/m^2 to −0.49 ± 0.14 W/m^2) has compensated about 70% of the increase in positive RF (from 0.09 ± 0.02 W/m^2 to 0.71 ± 0.11 W/m^2). This explains for the relatively slow increase in CHN's net contribution to the global RF over the 1949 to 2014 period (from 0.03 ± 0.02 W/m^2 to 0.22 ± 0.18 W/m^2). As for 2014, CHN's net RF was still less than half of that attributed to the United States, though the total of positive RF was close for the two countries.

Because of the different trends in positive, negative, and net RF, the relative contributions of the United States, EU15, and CHN to the global RF have shifted over the last 160 y (Fig. 2, *Insets*). The contribution of the United States to the global RF increased significantly before the 1960s (up to 21.9 ± 10.8%) and then remained stable with a slight decrease in the last decades. The EU15 overall trend has decreased (from 24.8 ± 11.1% to 13.7 ± 1.6%) over the past century, except the period 1970 to 1990 with a 1.5% increase. The relative contribution of CHN continuously decreased in the 1880 to 1980 period (from 8.2 ± 5.5% to 2.8 ± 6.1%) but had a recent increase from 1960 to 1970 (from 3.9 ± 7.3% to 4.3 ± 5.6%) when CHN's positive and negative RF both increased sharply. Since 1980, CHN's reforms and open policies have led to the current period of rapid economic growth, resulting over the last 30 y in an increasing relative contribution to the global RF (from 2.8 ± 6.1% to 8.6 ± 7.0%). Based on the time series of the absolute RFs contributed by CHN (Fig. 2*C*), the absolute values of RF are recategorized into well-mixed GHGs, warming SLCFs, and cooling SLCFs and for three periods 1880 to 1950, 1950 to 1980, and 1980 to 2014 (*SI Appendix*, Fig. S2). Positive RFs induced by well-mixed GHGs and warming SLCFs (mainly by BC and O_3t) increased five times, from 0.07 ± 0.02 W/m^2 in 1880 to 1950 to 0.44 ± 0.09 W/m^2 in 1980 to 2014. In the same periods, RF caused by cooling SLCFs in CHN increased from −0.02 ± 0.01 W/m^2 to −0.26 ± 0.16 W/m^2. The masked proportion of positive RF accounts for 28.6, 58.8, and 59.1% for three periods 1880 to 1950, 1950 to 1980, and 1980 to 2014 respectively.

Note that the relative contributions of the United States and EU15 to the global positive and negative RF simultaneously reached their peaks in the 1920s. At that same time, the United States and EU15 were contributing 30.4 ± 6.0% and 18.7 ± 3.4% to the global positive RF and 40.9 ± 11.1% and 15.3 ± 4.6% to the global negative RF, respectively. After the 1920s, these relative contributions started decreasing progressively in response to the growth of other economies in the world. Such synchronous increases in the relative contributions to both the global positive and negative RF are typical of the emerging economies, such as CHN after the 1980s. The consequence for these emerging economies is that they play an increasingly important role in changing global climate.

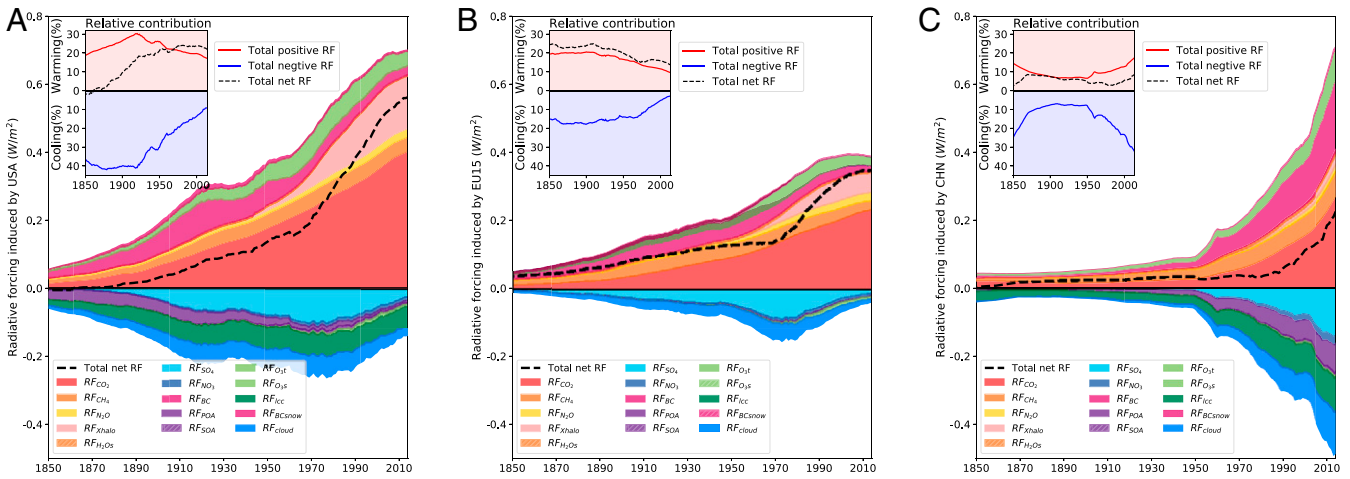

Fig. 2. Historical time series of the absolute RF contributions from the top three contributing regions. The positive and negative RF are stacked separately, and net RF are represented by the black dashed lines. The insets show the relative contribution of each region to global RF over the past three decades, including total of positive, negative, and net RF (*A*) for the United States, (*B*) for EU15, and (*C*) for CHN (including Mainland, Hong Kong, Macao, and Taiwan). Time series for other regions are presented in *SI Appendix*, Fig. S1.

Global RF Induced by the Five Aggregated Regions. Following Shared Socioeconomic Pathways, we group the abovementioned 15 regions into five aggregated regions, abbreviated as the Organization for Economic Co-operation and Development in 1990 (OECD), Asia countries (ASIA), Latin America and the Caribbean (LAM), MAF, and the Reforming Economies (REF) (*SI Appendix*, Table S1). These five aggregated regions are widely studied in the climate community; OECD is commonly regarded as a block of developed countries and the other four regions as developing countries. This system provides another perspective for evaluating the contributions to global RF.

OECD contributes 43.8 ± 3.7% (1.12 ± 0.10 W/m^2 out of 2.56 ± 0.58 W/m^2) to the global net RF (Fig. 3), which is proportional to its gross domestic product [GDP; 47.3%, 38,345.45 billion US dollars out of 81,002.42 billion US dollars in 2015 (16)] but much higher than its population share [15.8%, 1,140.78 million people out of 7,211.40 million people in 2015 (17)]. Relative contributions of ASIA, REF, LAM, and MAF to the global net RF are 21.1 ± 8.0%, 13.7 ± 2.4%, 8.9 ± 2.8%, and 12.5 ± 6.6%, respectively (Fig. 3). Note that ASIA contributes much less in comparison to its proportion of the global GDP [35.8% (16)] and of the population [52.8% (17)].

The high relative contribution of OECD to the global net RF is attributable to its high positive RF (1.41 ± 0.07 W/m^2) relative to its low negative RF (−0.29 ± 0.06 W/m^2). This small negative RF compensates for only 20.6% of the positive RF. In contrast, the compensations of the negative RF relative to the positive RF are 60.6% and 48.9% in ASIA and MAF, respectively (Fig. 3).

The composition of the RF is quite different among aggregated regions. Overall, the greatest contribution to the positive RF is from CO_2 emission, especially for OECD (57.4 ± 5.1%), LAM (55.6 ± 11.2%), and REF (54.5 ± 10.4%) (Fig. 3). Additionally, the contribution from halogenated compounds is pronounced for OECD (19.3 ± 0.9%). Note that the contributions from BC are also significant for ASIA (27.0 ± 8.4%) and for MAF (22.4 ± 3.5%).

The dominant contributors to the negative RF (Fig. 3) are sulfate aerosols (15.0 to 39.4%) and aerosol–cloud interaction (20.1 to 33.1%). For ASIA, MAF, and LAM, the contribution from POA is also important, accounting for 23.4 ± 8.3%, 29.8 ± 7.0%, and 15.3 ± 7.0%, respectively. LCC contributes the most to the negative RF in OECD (37.2 ± 16.9%) and LAM (32.7 ± 19.8%) through albedo effects, while it contributes noticeably to positive RF in MAF (16.0 ± 21.7%).

Discussion

This study examines the absolute and relative contributions of individual countries and aggregated regions or economies to the global RF.

Regional CO_2 emission dominates the positive RF for most countries. Halogenated compounds contribute significantly to the positive RF of developed countries, whereas CH_4, BC, and O_3t are important contributors in developing countries. Negative RF is mostly caused by sulfate aerosols and aerosol–cloud interactions, but POAs are also important for ASIA and MAF. LCC-induced RF can be negative or positive, depending on the type of biomes change (*SI Appendix*, Fig. S4).

This study includes another three RF components that were missing in a previous study of CHN's contribution to the global RF (3), making this assessment more comprehensive. The inclusion of SOA and BC deposition on snow slightly influenced the relative contributions of regions. However, inclusion of the aerosol–cloud interactions has a much larger impact, largely reducing CHN's relative contribution to the global RF (from 10 ± 4% in 2010 to 8.6 ± 7.0% in 2014). Moreover, the negative RF induced by the aerosol–cloud interactions accounts for 30.3% of the global negative RF (−0.46 ± 0.24 W/m^2 out of −1.52 ± 0.41 W/m^2) and is calculated with a large uncertainty (52%), increasing the uncertainty of CHN's relative contribution to the global RF (from 40 to 81%). When the ESMs are used in OSCAR in the form of different parameterizations, no ESM is excluded, rated, or weighted by skills in our Monte Carlo ensemble (n = 3,000). Although the global RF is bias corrected, the relative contribution of each region to global RF is not. Thus, the final uncertainty in the regional estimates is the combination of two factors: the diverging representation of regional processes among ESMs and the uncertainty in the driving data, that which remains quite high for short-lived pollutant datasets. Unlike the well-known GHG-induced RFs, the uncertainties of aerosol RFs are still large, especially when aerosol–cloud interactions are included (18). In global modeling, the uncertainties of RF_{SO_4} are reported at the level 34% [−0.32 ± 0.11 W/m^2 (19)], and the uncertainties of RF_{SO_4} range from 25 to 40% [0.23 ± 0.09 W/m^2 (19) to 0.84 ± 0.21 W/m^2 (20)]. The RF induced by aerosol–cloud interactions are evaluated in a broader range (−0.22 to −1.46 W/m^2, 5 to 95% CI) (21). For an individual region, the higher proportion of RF induced by aerosols, the larger uncertainty in its relative contribution to the global RF. In particular,

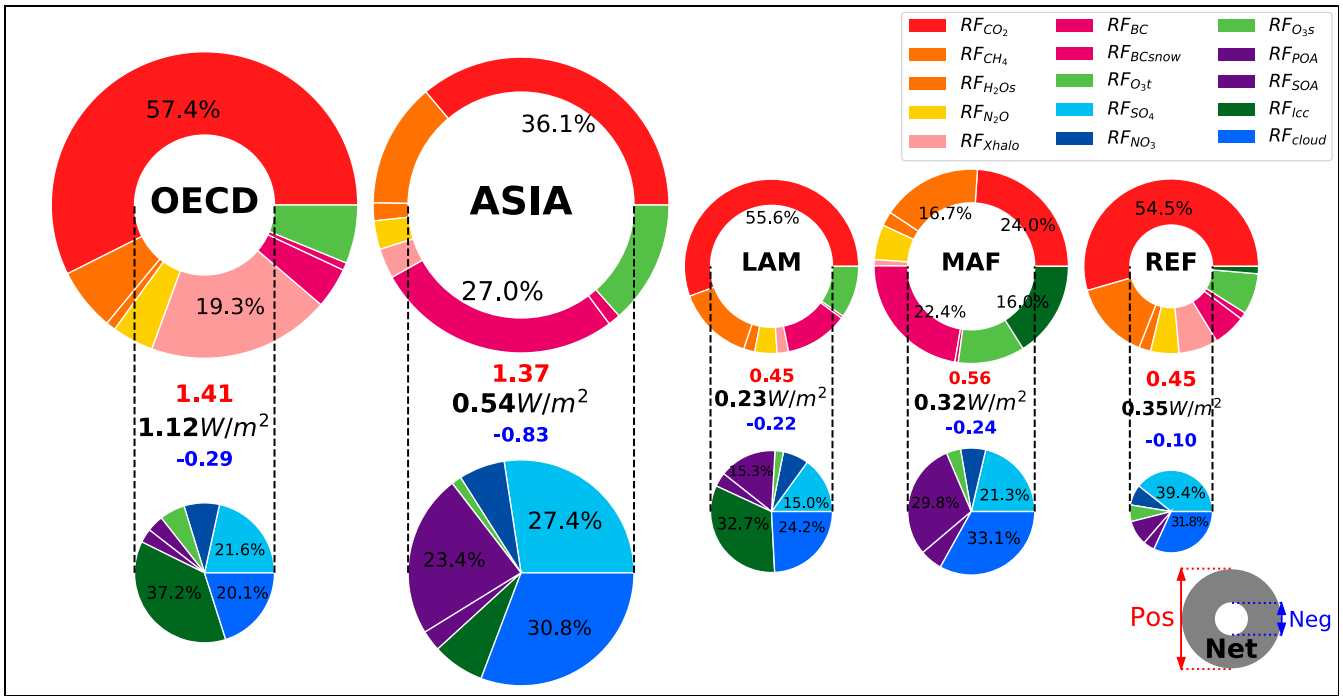

Fig. 3. RF composition of the five aggregated regions. The five aggregated regions are OECD, ASIA, LAM, MAF, and REF. For each aggregated region, total positive RF is proportional to the area of the larger circle. The blank inner circles represent the offsets of the negative RF, which composition is shown in the lower circle. The ring's area represents the net RF for each region.

the uncertainties of the regions heavily affected by aerosols, such as CHN, BRA, IND, and MAF, exceeded 50%, while the uncertainties of the regions with few aerosols, such as the United States, EU15, and JPN, are about 15% (Fig. 1*B*). It is therefore a priority to reduce the uncertainties of the RF induced by the aerosol–cloud interactions to make more accurate predictions of regional relative contributions. Nevertheless, the results of this study are consistent with Ward et al. (22) in evaluating the relative contributions of the United States and of CHN.

We note that the compensation effect of negative and positive RF found in our study is consistent with that of Skeie et al. (23) and Murphy et al. (14). The near-cancellation positive and negative RF in the EU15 during 1950 to 1970 and CHN during 1980 to 2000 are typical of periods with rapid development when less strict air quality controls are enforced. However, as the standard of living improves in developing countries, air quality under measures will be taken to combat pollution, causing a reduction in short-lived components. This reduction of the short-lived components will trigger a reduction of the current negative RF induced by sulfate aerosols and by aerosol–cloud interactions. It remains to be determined to what extent other air pollutants with warming potential, such as BC and ozone precursors, will be reduced, thereby impacting the contributions of developing countries to the global RF. Note that GHGs and SLCFs change the climate in an asymmetric way since GHGs stay in the atmosphere for a long time, while SLCFs can disappear rapidly after cessation of the source activities. Consequently, implementation of air quality policies will have a rapid impact on the total RF, but the RF change caused by GHG mitigation are slow to take effect. Therefore, considering the climate impact of air quality policies, more aggressive GHG reduction measures should be considered to achieve the temperature target. Moreover, short-lived species also have a smaller but longer-term effect on the climate system through climate–carbon feedback, as we recently quantified also with the OSCAR model (24). Thus, evaluating the contributions of developing countries to the future global RF is worthy of a continuous effort.

Methods

Model and Data. In this study, a compact ESM, OSCAR v3.1, is used to estimate anthropogenic RF and attribute them to countries and regions (4–6). OSCAR includes all the components of the Earth system necessary to simulate climate change: terrestrial and ocean carbon cycles, tropospheric and stratospheric chemistry, albedo changes, and climate responses. OSCAR has already been used in previous climate change attribution studies (3, 8, 9).

In addition, OSCAR is designed to emulate the sensitivity of higher resolution or complexity models as a metamodel. OSCAR v3.1 is trained on a large ensemble of ESMs and can be emulated on a specific ESM, which are listed in the description paper appendix B of the earlier v2.2 (4). Notably, the ocean carbon cycle was trained on four CMIP5 models, the land carbon cycle on seven CMIP5 models and 11 TRENDY v7 models, the climate response on 25 CMIP5 models, tropospheric O_3 on nine Atmospheric Chemistry and Climate Model Intercomparison Project (ACCMIP) models, the direct aerosols effects on four CMIP5 models and 15 AeroCom2 models, and the indirect aerosols effect on five ACCMIP models. Here, OSCAR is used in a probabilistic framework, that is, parameters are randomly drawn from the pool of available configurations, which are calibrated on the complex ESMs.

The model and the input datasets used in this study are available at https://github.com/tgasser/OSCAR/releases/tag/v3.1. The input data are emissions of GHGs, emissions of ozone precursors and aerosols, and land-use change. The datasets are all available online and originated from the Carbon Dioxide Information Analysis Center (25), the Emissions Database for Global Atmospheric Research (26), the Community Emissions Data System (27), the emission module of the Potsdam Real-time Integrated Model for the probabilistic Assessment of emission Paths (28), and LUH2 (11). Part of the uncertainties of our results come from the variances of the datasets.

RF Constraints. The global RF estimated by OSCAR v3.1 is constrained by the RF in year 2011 reported in IPCC AR5 (2). We calculate scale factors for species in Table 1 by using chapter 8 SM of IPCC AR5 (2). The scale factors are calculated with $f_i = \frac{RF_i^{OSCAR}}{RF_i^{IPCC}}$ and applied to the time series. The results with constraints are close to that in IPCC AR5 (*SI Appendix*, Fig. S5).

Attribution Method. In this study, the normalized marginal attribution method is used to attribute global RF to countries and regions. In our previous work for CHN's climate contribution, this method is applied (3). The attribution method isolated relative contributions to climate change of countries and regions according to their marginal effect of emissions to global RF, which is advised by the UNFCCC (29).

To attribute global RF induced by component X (RF_x) to m regions,

m + 1 simulations are needed. First, a "normal" simulation with all emissions is run to obtain $RF_X = OSCAR(E_{globe})$. Then, one simulation with regional emissions reduced by a small fraction (ε) is run for each region i to obtain $`RF_x^i = OSCAR(E_{globe} - \varepsilon E_i)$. Here, we obtain the marginal effect of each region, which is$\Delta_i RF_X = RF_X - `RF_x^i = OSCAR(E_{globe}) - OSCAR(E_{globe} - \varepsilon E_i)$. Last, the regions' relative contributions are deduced by normalization: $\alpha_i = \frac{\Delta_i RF_X}{\sum_{i=1}^{m} \Delta_i RF_X}$. For OSCAR, ε value is used as 0.1%. Studies have found that the attribution results are virtually not sensitive to the ε value as long as it remains fairly small (7, 29). To obtain the absolute contributions induced by regions, we multiply their relative contributions with global RF: $RF_X^i = \alpha_i RF_X$.

Uncertainty Analysis. In this study, we use a Monte Carlo ensemble ($n = 3{,}000$) for parameters and driver datasets to obtain uncertainties. As mention above, here, OSCAR is used in a probabilistic framework. Parameters are randomly drawn from the pool of available configurations, which are calibrated from different ESMs. In addition, driver datasets are from different origins. Parameters and driver datasets are combined randomly for the Monte Carlo element. The average values of the Monte Carlo simulation results are regarded as our best estimates, and the SDs are regarded as uncertainties.

Data Availability. All study data are included in the article and/or *SI Appendix*.

ACKNOWLEDGMENTS. This study is supported by the National Natural Science Foundation of China Grants 41771495, 41830641, and 41988101 and the Second Tibetan Plateau Scientific Expedition and Research Program Grant 2019QZKK0208. Development of OSCAR v3.1 is funded by the European Research Council Synergy project "Imbalance-P" (Grant ERC-2013-SyG-610028) and European Union's Horizon 2020 research and innovation project "CONSTRAIN" (Grant #820829).

1. R. K. Pachauri and L. A. Meyer, Climate Change 2014: Synthesis Report (IPCC, Geneva, Switzerland, 2014).
2. T. F. Stocker *et al*., "Anthropogenic and natural radiative forcing" in *Climate Change 2013: The Physical Science Basis. Contribution of Working Group I to the Fifth Assessment Report of the Intergovernmental Panel on Climate Change*, P. M. Midgley, Ed. (Cambridge University Press, Cambridge, United Kingdom and New York, NY, 2013), p. 1535.
3. B. G. Li *et al*., The contribution of China's emissions to global climate forcing. *Nature* **531**, 357–361 (2016).
4. T. Gasser *et al*., The compact Earth system model OSCAR v2.2: Description and first results. *Geosci. Model Dev.* **10**, 271–319 (2017).
5. T. Gasser *et al*., Path-dependent reductions in CO2 emission budgets caused by permafrost carbon release. *Nat. Geosci.* **11**, 830–835 (2018).
6. T. Gasser *et al*., Historical CO2 emissions from land-use and land-cover change and their uncertainty. *Biogeosciences Discuss.* 10.5194/bg-2020-33 (2020).
7. N. Hohne *et al*., Contributions of individual countries' emissions to climate change and their uncertainty. *Clim. Change* **106**, 359–391 (2011).
8. P. Ciais *et al*., Attributing the increase in atmospheric CO2 to emitters and absorbers. *Nat. Clim. Chang.* **3**, 926–930 (2013).
9. G. Shen *et al*., Impacts of air pollutants from rural Chinese households under the rapid residential energy transition. *Nat. Commun.* **10**, 3405 (2019).
10. V. Eyring *et al*., Overview of the Coupled Model Intercomparison Project Phase 6 (CMIP6) experimental design and organization. *Geosci. Model Dev.* **9**, 1937–1958 (2016).
11. G. Hurtt *et al*., *Harmonization of global land use scenarios (LUH2): Historical v2.1h 850 - 2015*. Earth System Grid Federation (2017). https://doi.org/10.22033/ESGF/input4MIPs.1127.
12. G. C. Hurtt *et al*., Harmonization of global land use change and management for the period 850–2100 (LUH2) for CMIP6. *Geosci. Model Dev.* **13**, 5425–5464 (2020).
13. G. C. Hurtt *et al*., Harmonization of land-use scenarios for the period 1500-2100: 600 years of global gridded annual land-use transitions, wood harvest, and resulting secondary lands. *Clim. Change* **109**, 117–161 (2011).
14. D. M. Murphy, A. R. Ravishankara, Trends and patterns in the contributions to cumulative radiative forcing from different regions of the world. *Proc. Natl. Acad. Sci. U.S.A.* **115**, 13192–13197 (2018).
15. National Bureau of Statistics, "Gross domestic product index since 1978" ('National Accounts' for GDP, National Bureau of Statistics of China, 2014). https://data.stats.gov.cn/english/easyquery.htm?cn=C01. Accessed 20 March 2021.
16. J. C. Cuaresma, Income projections for climate change research: A framework based on human capital dynamics. *Glob. Environ. Change* **42**, 226–236 (2017).
17. S. Kc, W. Lutz, The human core of the shared socioeconomic pathways: Population scenarios by age, sex and level of education for all countries to 2100. *Glob. Environ. Change* **42**, 181–192 (2017).
18. C. J. Smith *et al*., Effective radiative forcing and adjustments in CMIP6 models. *Atmos. Chem. Phys.* **20**, 9591–9618 (2020).
19. G. Myhre *et al*., Radiative forcing of the direct aerosol effect from AeroCom Phase II simulations. *Atmos. Chem. Phys.* **13**, 1853–1877 (2013).
20. T. C. Bond *et al*., Bounding the role of black carbon in the climate system: A scientific assessment. *J. Geophys. Res. D Atmospheres* **118**, 5380–5552 (2013).
21. N. Bellouin *et al*., Bounding global aerosol radiative forcing of climate change. *Rev. Geophys.* **58**, e2019RG000660 (2020).
22. D. S. Ward, N. M. Mahowald, Contributions of developed and developing countries to global climate forcing and surface temperature change. *Environmental Research Letters* **9**, 074008 (2014).
23. R. B. Skeie *et al*., Perspective has a strong effect on the calculation of historical contributions to global warming. *Environ. Res. Lett.* **12**, 024022 (2017).
24. B. Fu *et al*., Short-lived climate forcers have long-term climate impacts via the carbon-climate feedback. *Nat. Clim. Chang.* **10**, 851–855 (2020).
25. T. A. Boden, G. Marland, R. J. Andres, *Global, Regional, and National Fossil Fuel CO2 Emissions* (Carbon Dioxide Information Analysis Center, Oak Ridge National Laboratory, U.S. Department of Energy, 2017).
26. M. Crippa *et al*., Gridded emissions of air pollutants for the period 1970-2012 within EDGAR v4.3.2. *Earth Syst. Sci. Data* **10**, 1987–2013 (2018).
27. R. M. Hoesly *et al*., Historical (1750-2014) anthropogenic emissions of reactive gases and aerosols from the Community Emissions Data System (CEDS). *Geosci. Model Dev.* **11**, 369–408 (2018).
28. J. Gütschow *et al*., The PRIMAP-hist national historical emissions time series. *Earth Syst. Sci. Data* **8**, 571-603 (2016).
29. United Nations Framework Convention on Climate Change (UNFCCC). Methodological Issues: Scientific and Methodological Assessment of Contributionsto Climate Change, Report of the Expert Meeting, Note by the Secretariat (UNFCCC, 2002). http://unfccc.int/resource/docs/2002/sbsta/inf14.pdf.